AD-A248 622

(2)

TECHNICAL REPORT BRL-TR-3322

BRL

PRESSURE OSCILLATIONS DURING THE INTERIOR BALLISTIC FIRING OF REGENERATIVE LIQUID PROPELLANT GUNS

J. D. KNAPTON
C. A. WATSON
N. E. BOYER

MARCH 1992

APPROVED FOR PUBLIC RELEASE; DISTRIBUTION IS UNLIMITED.

U.S. ARMY LABORATORY COMMAND

BALLISTIC RESEARCH LABORATORY
ABERDEEN PROVING GROUND, MARYLAND

NOTICES

REPORT DOCUMENTATION PAGE

Form Approved
OMB No. 0704-0188

1. AGENCY USE ONLY (*Leave blank*)	2. REPORT DATE	3. REPORT TYPE AND DATES COVERED
	March 1992	Final, Jan 85 - May 86

4. TITLE AND SUBTITLE

Pressure Oscillations During the Interior Ballistic Firing of Regenerative Liquid Propellant Guns

5. FUNDING NUMBERS

PR: 1L263637D155

6. AUTHOR(S)

J.D. Knapton, C.A. Watson, and N.E. Boyer

7. PERFORMING ORGANIZATION NAME(S) AND ADDRESS(ES)

8. PERFORMING ORGANIZATION REPORT NUMBER

9. SPONSORING/MONITORING AGENCY NAME(S) AND ADDRESS(ES)

U.S. Army Ballistic Research Laboratory
ATTN: SLCBR-DD-T
Aberdeen Proving Ground, MD 21005-5066

10. SPONSORING/MONITORING AGENCY REPORT NUMBER

BRL-TR-3322

11. SUPPLEMENTARY NOTES

This report is based on a paper given at the 22nd JANNAF Combustion Meeting, October 1985.

12a. DISTRIBUTION/AVAILABILITY STATEMENT

Approved for public release; distribution is unlimited.

12b. DISTRIBUTION CODE

13. ABSTRACT *(Maximum 200 words)*

Pressure oscillation data from 25-mm and 30-mm regenerative injection liquid propellant gun tests are examined and interpreted in terms of acoustical instabilities. Data from one test with the 30-mm suggest that the observed frequencies are consistent with sound speeds between 976 m/s and 1,009 m/s. For comparison, the thermodynamic computed sound speed, based on a BLAKE calculation and assuming a 10% heat loss, is 1,134 m/s. Also, a mean sound speed computed from the RLPG model by Terence Coffee of the Ballistic Research Laboratory and assuming delayed burning is 967 m/s.

14. SUBJECT TERMS

liquid propellants; regenerative injection gun; acoustical instabilities; sound speed; liquid gun propellants

15. NUMBER OF PAGES

44

16. PRICE CODE

17. SECURITY CLASSIFICATION OF REPORT	18. SECURITY CLASSIFICATION OF THIS PAGE	19. SECURITY CLASSIFICATION OF ABSTRACT	20. LIMITATION OF ABSTRACT
UNCLASSIFIED	UNCLASSIFIED	UNCLASSIFIED	UL

INTENTIONALLY LEFT BLANK.

TABLE OF CONTENTS

INTENTIONALLY LEFT BLANK.

LIST OF FIGURES

Figure | Page

LIST OF TABLES

INTENTIONALLY LEFT BLANK.

1. INTRODUCTION

The regenerative liquid-propellant gun (RLPG) used in this study is of the Concept VI type, Figure 1 (Mandzy, Cushman, and Magoon 1984a, 1984c, 1984d; Reeves 1985; Pate and Magoon 1985; Magoon et al. 1985). This design uses an in-line annular, regenerative piston to pump a monopropellant into the combustion chamber where the propellant breaks up into droplets and burns. The concept has been studied at General Electric, Pittsfield, MA, in 25-mm (Mandzy, Cushman, and Magoon 1984a, 1984d), 30-mm (Mandzy, Cushman, and Magoon 1984a; Reeves 1985; Pate and Magoon 1985; Magoon et al. 1985), and 105-mm (Mandzy, Cushman, and Magoon 1984a, 1984c; Mandzy et al. 1983, Morrison and Knapton 1984) test fixtures, and a version of the Concept VI RLPG is being tested at the U.S. Army Ballistic Research Laboratory (BRL), Aberdeen Proving Ground, MD (Magoon et al. 1985; Watson et al. 1985; Watson et al. 1986; Watson, Knapton, and Klein 1987; Klingenberg et al. 1987). Pressure records from tests with the Concept VI type fixtures typically show high-frequency oscillations. Based on research in liquid-propellant rocket engines, high-frequency oscillations account for many problems such as increased heat transfer, mechanical vibration, or abnormally high pressure spikes. These concerns are not addressed in this paper; instead, we will assume that the oscillations are of acoustical origin and consider only the nature of the oscillations and not their effect on the system. Interestingly, if the oscillations are of acoustical origin, then an identification of the acoustical modes permits a means for estimating the sound speed in the chamber. Therefore, estimates of the sound speed will be given and compared with values determined from both the BLAKE thermochemical code (Freedman 1987) and an interior ballistic model (Coffee 1985, 1986).

Kent (1936) was one of the first investigators who used the sound speed to interpret pressure data measured during the combustion of a solid propellant in a closed chamber. Kent was able to obtain an estimate for the specific heat of the combustion gases by assuming a value for the sound speed in the chamber. More recently, Juhasz (1987) has interpreted, in terms of a sound speed, pressure oscillations that occur during the combustion of solid propellants in closed chambers.

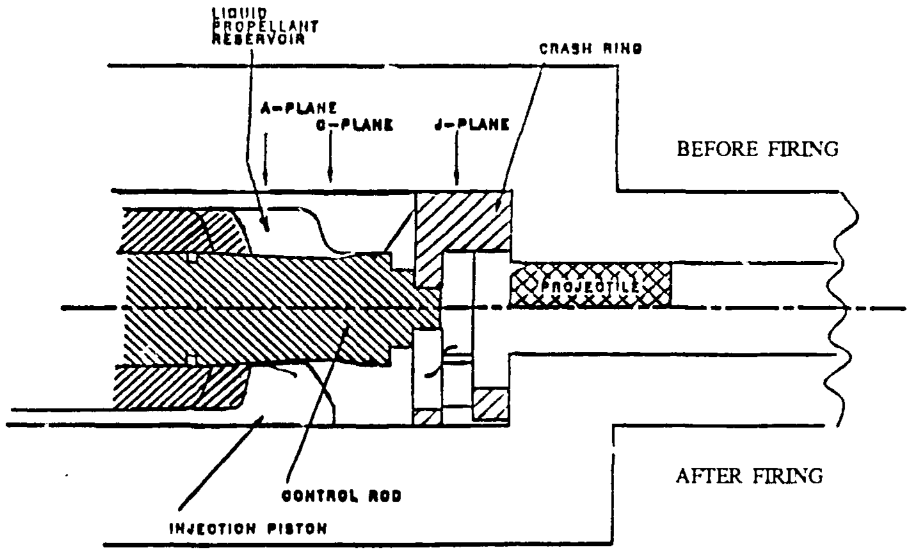

Figure 1. Concept VI, In-Line Annular Piston, 1/3 Charge Configuration.

Two important observations are noted from the earlier RLPG studies (Magoon et al. 1985; Watson et al. 1985). First, it was shown (Magoon et al. 1985) that analog data, Figure 2, from one of the tests yielded a rather well-defined frequency, which remained approximately constant throughout the interior ballistic cycle. A constant frequency can suggest a constant sound speed. An approximately constant frequency could also be explained by other mechanisms, such as by compensating effects between changes in the complex two-phase flow, by temperature effects, and by changes in geometry. However, the assumption of constant sound speed yields an interesting and relatively simple basis for estimating the sound speed, which may be of some merit. Also, an earlier study (Watson et al. 1985) using a modified chamber insert, Figure 3, in a configuration that more closely approaches the shape of a cylindrical chamber, resulted in significant variations in the nature of the oscillations. Changes in the chamber geometry would have a direct influence in the generation of the observed frequencies, provided the frequencies are related to the assumed acoustical modes.

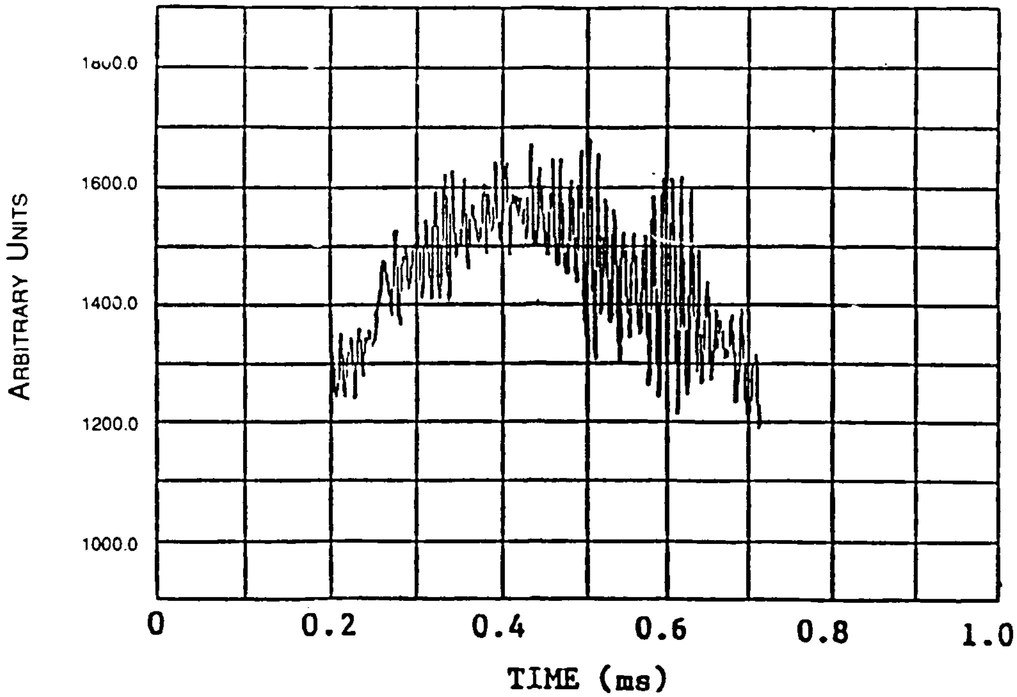

Figure 2. Example of Chamber Pressure-Time Data Digitized at 400 kHz, LGP 1846, J Plane.

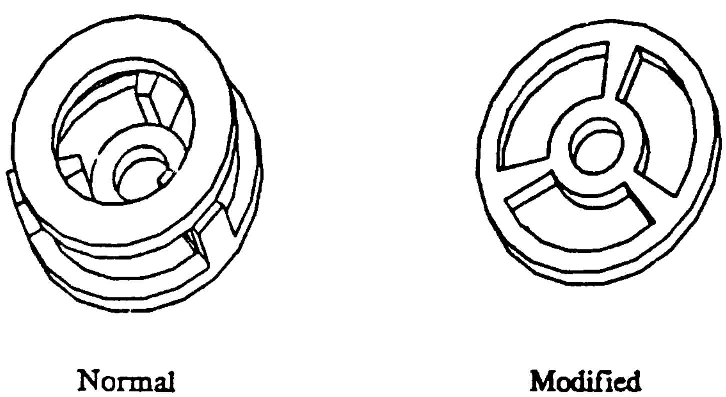

Figure 3. Illustration of Modified Crash Ring and Normal Crash Ring.

2. BACKGROUND

2.1 Propellant. The liquid propellant used in the recent studies is the hydroxylammonium nitrate (HAN) based monopropellant, designated LGP 1846. A summary of its thermochemistry properties, along with LP 1845 for comparison purposes, is given in Table 1. Earlier studies used Otto-II, a monopropellant with a lower impetus than the HAN-based monopropellants. The properties of Otto-II are also included in Table 1.

Table 1. Properties of the Liquid Propellants Used in the Gun Firings[a]

LP name	Fuel name	Composition			Density, g/cm^3	Impetus, J/g	Flame temp., K	Gamma
		Fuel, Wt%	HA* Wt%	Water, Wt%				
1845	TEAN	20.0	63.2	16.8	1.46	934	2,592	1.218
1846	TEAN	19.2	60.8	20.0	1.42	898	2,469	1.223
Otto-II	—	—	—[b]	—	1.23	866	1,986	1,266

[a]Thermochemical calculations for a loading density = 0.2 g/cc (Freedman 1987).

[b]Composition of Otto-II: 76% 1,2 dinitroxypropane, 22.5% di-N-butyl sebacate, 1.5% 2 nitrodiphenylamine.

2.2 Test Fixtures. This study focuses on the Concept VI type of RLPG. However, two earlier RLPG concepts, tested in 25-mm and 40-mm fixtures, are briefly mentioned since these fixtures also exhibit pressure oscillations.*

2.2.1 Earlier RLPG Concepts.

(1) The 40-mm RLPG In-Line Showerhead Piston (Benet Weapons Laboratory [BWL], Watervliet, NY). One of the first RLPG fixtures that showed pressure oscillations was a 40-mm gun (Graham 1987) tested at BWL (Hasenbein 1981). This gun used an in-line piston with a showerhead-type injector similar to some of the early concepts tested at General

*It should be noted that tests with some medium-caliber RLPG fixtures have resulted in pressure records, which did not show any oscillations. One fixture, tested at the General Electric Armament Systems Division, Burlington, VT (Graham and Bulman 1975), was a 25-mm RLPG with a showerhead-type piston face. Other fixtures, tested at the General Electric Ordnance Systems Division, Pittsfield, MA, have been 30-mm RLPG fixtures similar to the Concept VI described in this report, but with various changes in the orifice injection geometry.

Electric (Graham and Bulman 1975). Otto-II was injected during the interior ballistic cycle through holes drilled in the head of the piston. This concept was dropped due to the difficulty in initially sealing the propellant and to a lack of control in the mass injection rate during the interior ballistic cycle.

The 40-mm BWL fixture exhibited a high-frequency (11 kHz) acoustical instability in the chamber, which was interpreted as the first tangential mode (Hasenbein 1981; Graham 1982). This instability was initiated when the piston was displaced a distance approximately equal to the chamber diameter. The amplitude of the oscillations was reduced, but not eliminated, by contouring the piston face to resemble baffles.

(2) The 25-mm Concept V (General Electric Ordnance Systems Division). Pressure oscillations were also recorded with a different type of injection concept. In this concept, the propellant was initially confined between an axial hollow rod and the chamber wall (Mandzy, Cushman, and Magoon 1984b). Otto-II was injected during the interior ballistic cycle through holes drilled in the wall of the hollow rod. In some cases, the propellant was also injected through an annulus around the outside of the head of the piston. In this case, the propellant was in contact with the inner wall of the chamber. This concept offered a means for initially sealing the propellant reservoir and varying the mass injection rate.

A major concern in the test results with Concept V was the presence of large-amplitude, high-frequency oscillations present in the pressure-time records (Mandzy, Cushman, and Magoon 1984a, 1984b). The frequencies of the oscillations were 10–50 kHz and persisted well past injection. The oscillations had the maximum amplitudes at the face of the piston and chamber wall. Attempts to correct the problem failed. This concept was later abandoned due to problems not associated with the oscillations.

2.2.2 Concept VI.

(1) Description. The Concept VI-type fixture (Figure 1) has been tested in 25-mm (Mandzy, Cushman, and Magoon 1984a, 1984d), 30-mm (Mandzy, Cushman, and Magoon 1984a; Reeves 1985; Pate and Magoon 1985; Magoon et al. 1985; Watson et al. 1985, 1986; Watson, Knapton, and Klein 1987; Klingenberg et al. 1987), and 105-mm

(Mandzy, Cushman, and Magoon 1984a, 1984c; Mandzy et al. 1983; Morrison and Knapton 1984) gun fixtures. These fixtures inject propellant into the combustion chamber in the form of an annular sheet. An illustration of the basic concept showing both the chamber and LP reservoir sections is given in Figure 1. In the upper half of the figure, the piston is in the forward position prior to firing. The lower half of the figure shows the piston in the rear position at the end of firing. The piston is a thin-shell cylinder supported from deformation by a lubricating film and the chamber wall. At ignition, the pressure developed by the igniter in the combustion chamber forces the injection piston to the rear. Due to the differential area of the injection piston, the pressure in the reservoir is higher than in the combustion chamber. As a result, LP is forced through the annulus formed by the outside of the control rod, or center bolt, and the inner diameter of the piston. The injected propellant then enters the combustion chamber. The instantaneous injection area is controlled by contours on the control rod. Initially, the area is sealed, preventing leakage of LP into the chamber during LP fill and allowing for the prepressurization of the LP reservoir. For the tests reported here, the initial prepressurization of the LP was 7.0 MPa. As the injection piston is displaced to the rear, the injection area rapidly increases, permitting an increase in the mass injection rate. Maximum injection area is reached at the end of the first or starting taper on the control rod. Motion of the injection piston is retarded toward the end of its stroke by the rear taper on the control rod.

A chamber insert, called a crash ring, Figure 3, was used in all of the tests. The purpose of the crash ring is to center the control rod; provide a stop for the piston during prepressurization; and provide a collapsible object, in the event the piston reverses, to minimize damage to the hardware.

(2) Concept VI, 25-mm, Test Conditions. The 25-mm RLPG was tested at the General Electric test facility, Malta, NY (Mandzy, Cushman, and Magoon 1984a, 1984d). Chamber pressures, the propellant reservoir pressure, the projectile velocity, and the piston velocity were recorded. The rear chamber pressure gage and the forward chamber pressure gage were located, respectively, 3.72 cm to the rear and 1.33 cm forward of the initial position of the piston face. Otto-II was used for the tests. The mean charge mass was 115 g, with a standard deviation of 0.29 g. The charge-mass-to-projectile-mass ratio (C/M) was 0.634. Illustrations of the forward and rear chamber pressures are shown in Figures 4 and 5, together

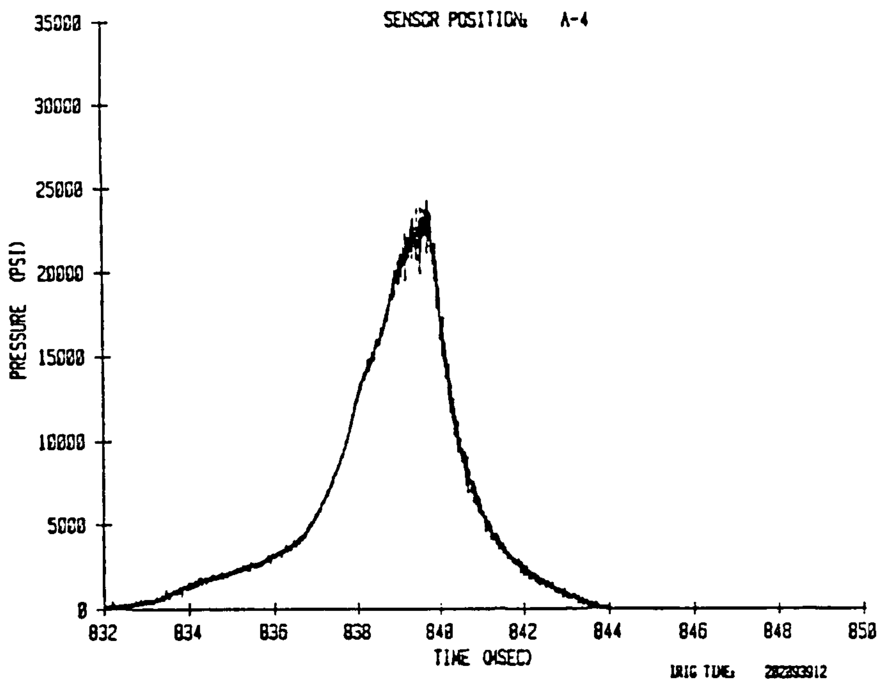

Figure 4. Forward Chamber Pressure-Time Plot for a 25-mm Firing Using Otto-II.

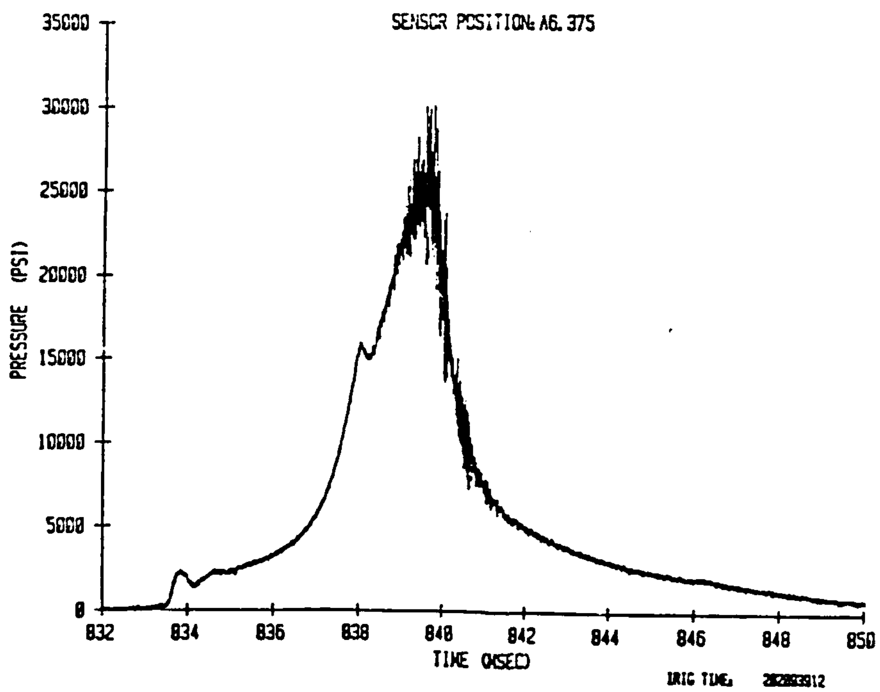

Figure 5. Rear Chamber Pressure-Time Plot for a 25-mm Firing Using Otto-II.

with the reservoir pressure, Figure 6, and the piston displacement (recorded by an optical tracker, commercially called an Optron), Figure 7. (The zero reference time in these plots is the time at the start of data recording. The pressure data from the propellant reservoir, Figure 6, is not expressed in engineering units, as the type of transducer used in the reservoir was a new miniature gage, and the gage mounting and calibration procedures had not been specified. The actual pressure deflection may be approximated by comparison with the scales of the other two gages shown in Figures 4 and 5.) In Figures 5 and 6, the oscillation at the start is associated with the response and injection of the propellant from the reservoir, and the pulse at about one-half of maximum pressure in Figure 5 is due to the uncovering of the gage by the piston. The response from the Optron, Figure 7, shows a smooth start-up and a gradual deceleration. (The total piston displacement in Figure 7 is about 58 mm).

- Pressure Oscillations. The responses of the pressure gages in the chamber show no evidence of oscillations until a pressure of 130 to 140 MPa is reached. The maximum amplitudes of the oscillations in the forward section of the chamber are about 6 to 12% of the maximum pressure, while the maximum amplitude of the oscillations in the rear of the chamber are about two times larger. The dominant frequency of the pressure oscillations in the chamber are in the 50- to 60-kHz range.

- Scaling Tests. Additional 25-mm tests were also performed at General Electric with the objective of investigating the effect of different sheet thicknesses on the interior ballistics. The results were to provide scaling information for designing a 105-mm Concept VI, RLPG (Mandzy, Cushman, and Magoon 1984a, 1984d). For these tests, the total injection area was the same as that used in the preceding example. However, the sheet thickness was not uniform. The nonuniform sheet thickness was achieved by machining scallops on the center bolt, Figure 8. The result was three regions of the sheet, which had thicknesses much larger than the sheet thickness used in the reproducibility group, while, at the same time, there were three other regions with sheet thicknesses that were much less. A description of the test configuration and results is given in Mandzy, Cushman, and Magoon (1984d). Briefly, the results yielded much larger pressure oscillations than those observed in the reproducibility group. One test group that was particularly interesting involved firing a projectile with twice the nominal projectile mass. The response of the pressure gage at the rear of the chamber is

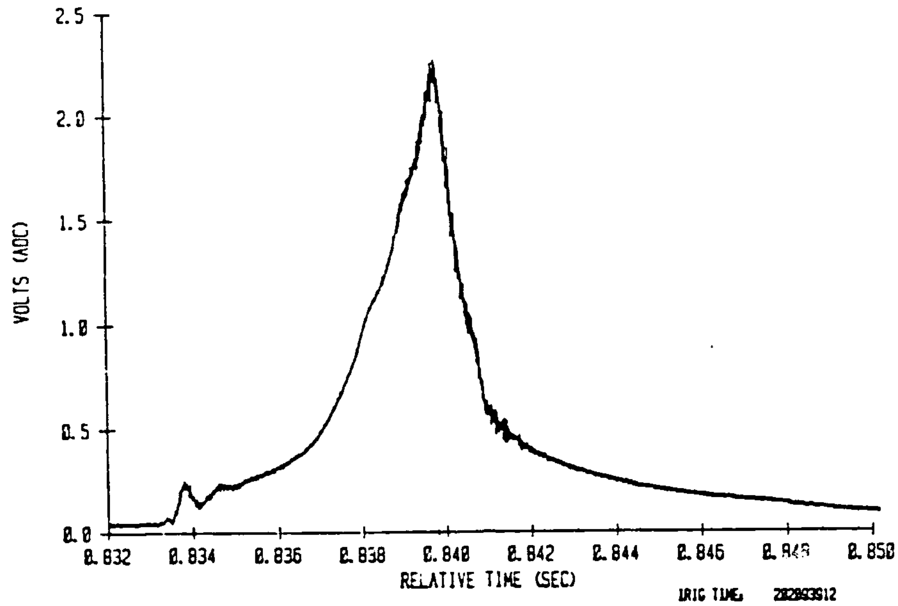

Figure 6. Propellant Reservoir Pressure-Time Plot for a 25-mm Firing Using Otto-II.

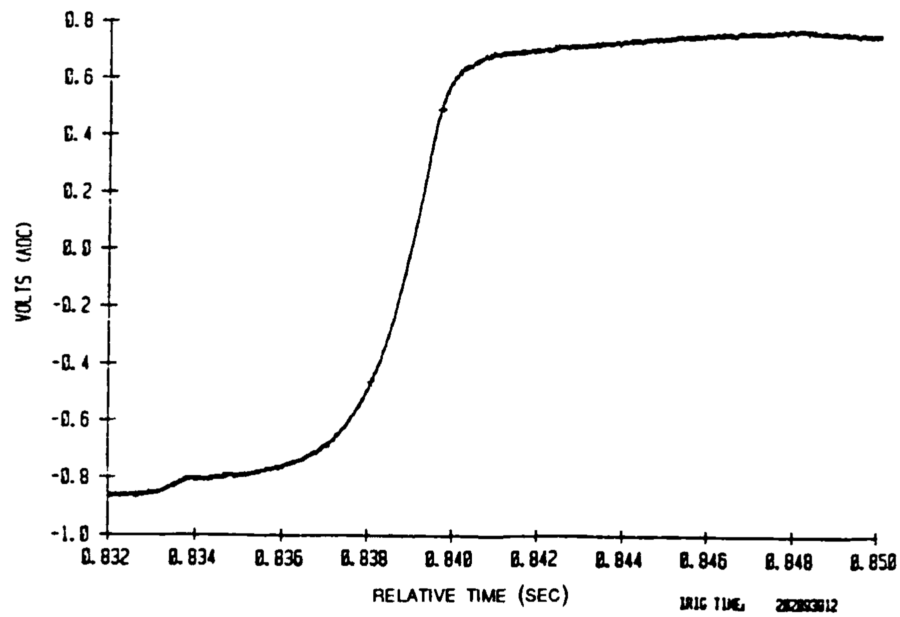

Figure 7. Piston Displacement Plot for a 25-mm Firing Using Otto-II.

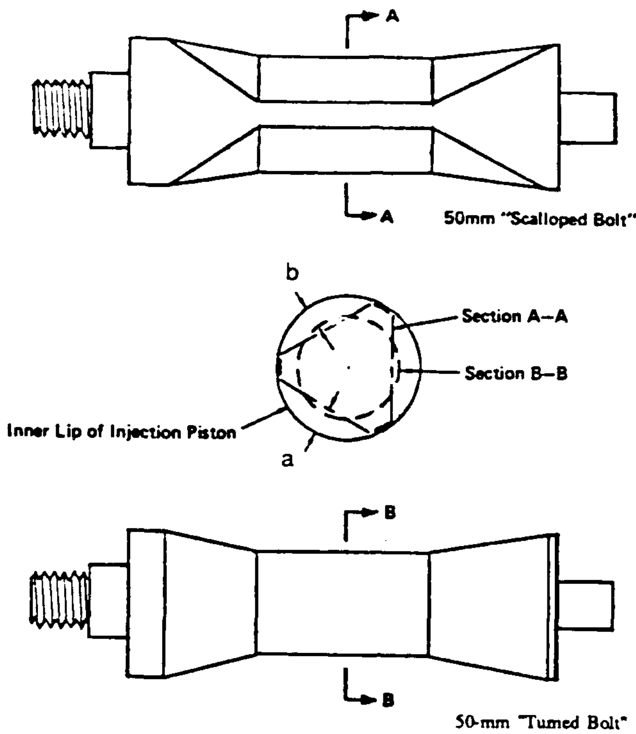

Figure 8. Illustration of Cross Section of a Control Rod Showing the Normal Circular Cross Section and the Scalloped Cross Section Used for the Scaling Tests.

shown in Figure 9. Figures 10–12 show the power spectral density plots of the pressure data for three time intervals during the pressure-vs.-time record. During the decay of the pressure, there is apparently an excitation of the acoustical modes in the chamber, as suggested by the occurrence of the high-order harmonics illustrated in Figure 12. The first peak occurs at 23.5 kHz, and the approximate frequency interval between the peaks is also about 23 kHz. The first radial mode, for a uniform center bolt and a sound speed of 701 m/s, is 23.9 kHz (Grachis 1983). The calculated second radial mode occurs at 44.7 kHz, which compares with the observed doublet with peaks at 45 and 48 kHz. Assuming a somewhat lower sound speed, of course, would improve the agreement. Also, the agreement could be improved by keeping the same sound speed and increasing the radial dimension due to the nonuniform center bolt. The observed frequencies (Figure 12) during the pressure decay occur when the piston is decelerating on the injection taper, and the injection sheet is becoming progressively thinner, probably producing a more rapid breakup and more localized burning of the propellant.

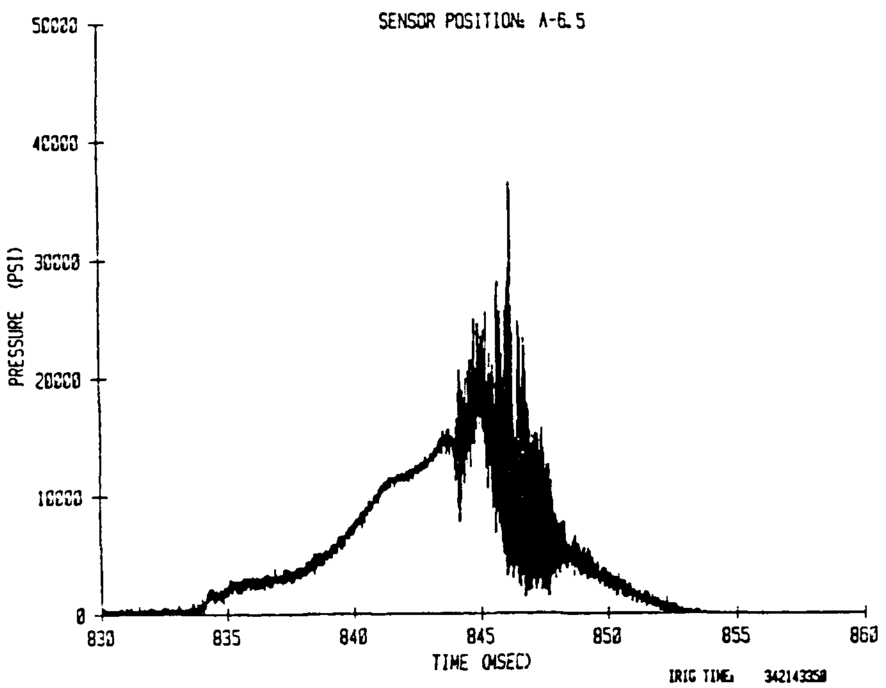

Figure 9. Chamber Pressure-Time Plot for a 25-mm Firing With Otto-II and With a Nonuniform Propellant Injection Sheet (I.D. No. 342.14.33.50).

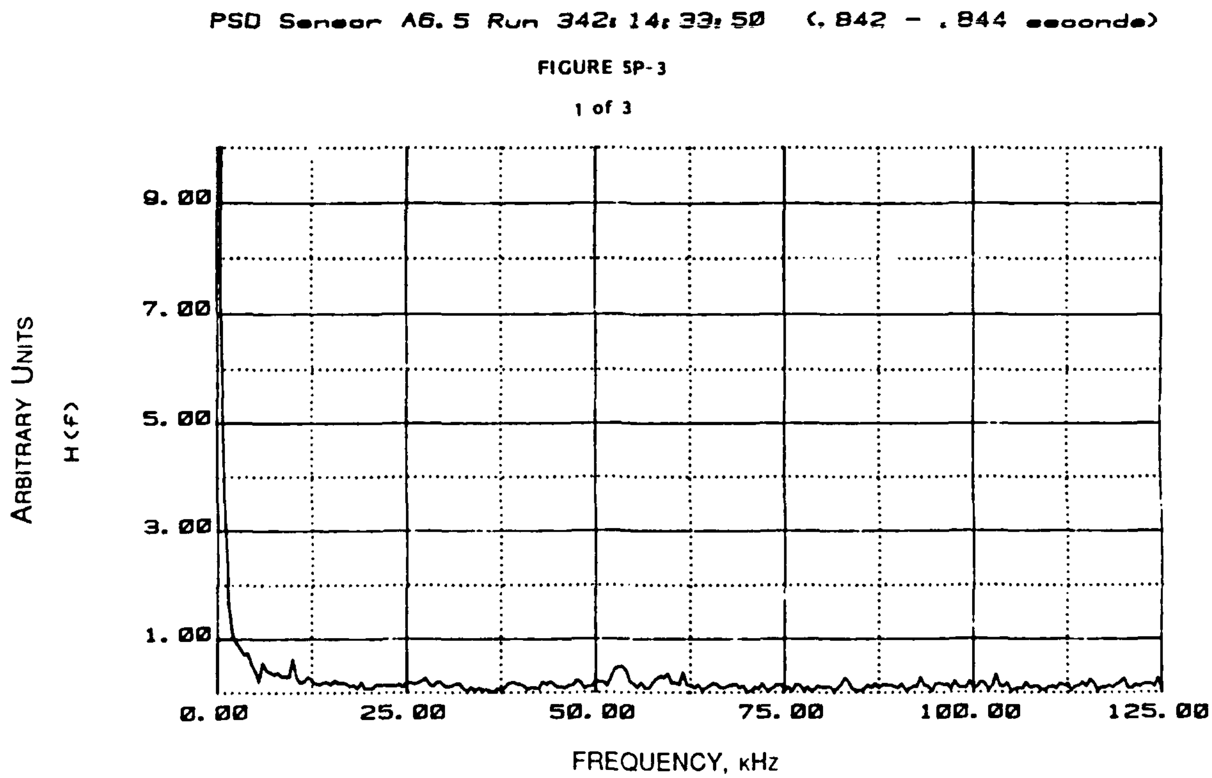

Figure 10. Frequency Analysis Plot, I.D. No. 342.14.33.50, From 842 to 844 ms.

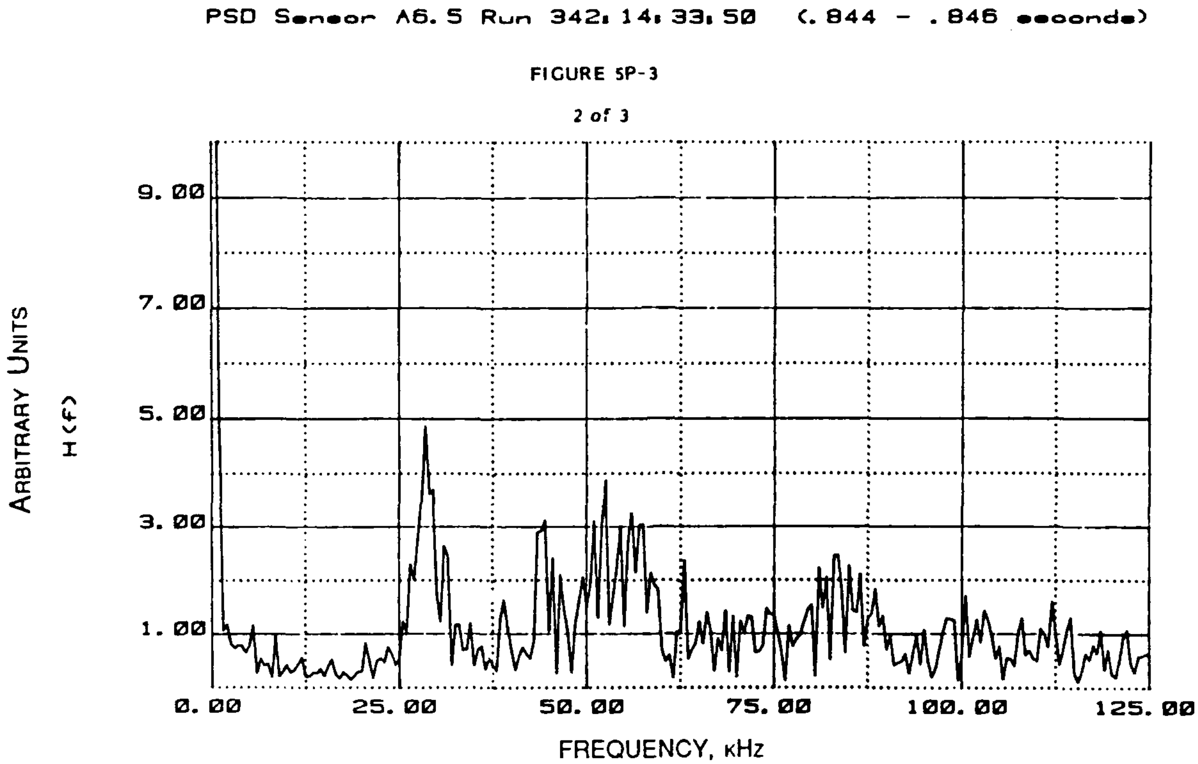

Figure 11. Frequency Analysis Plot, I.D. No. 342.14.33.50, From 844 to 846 ms.

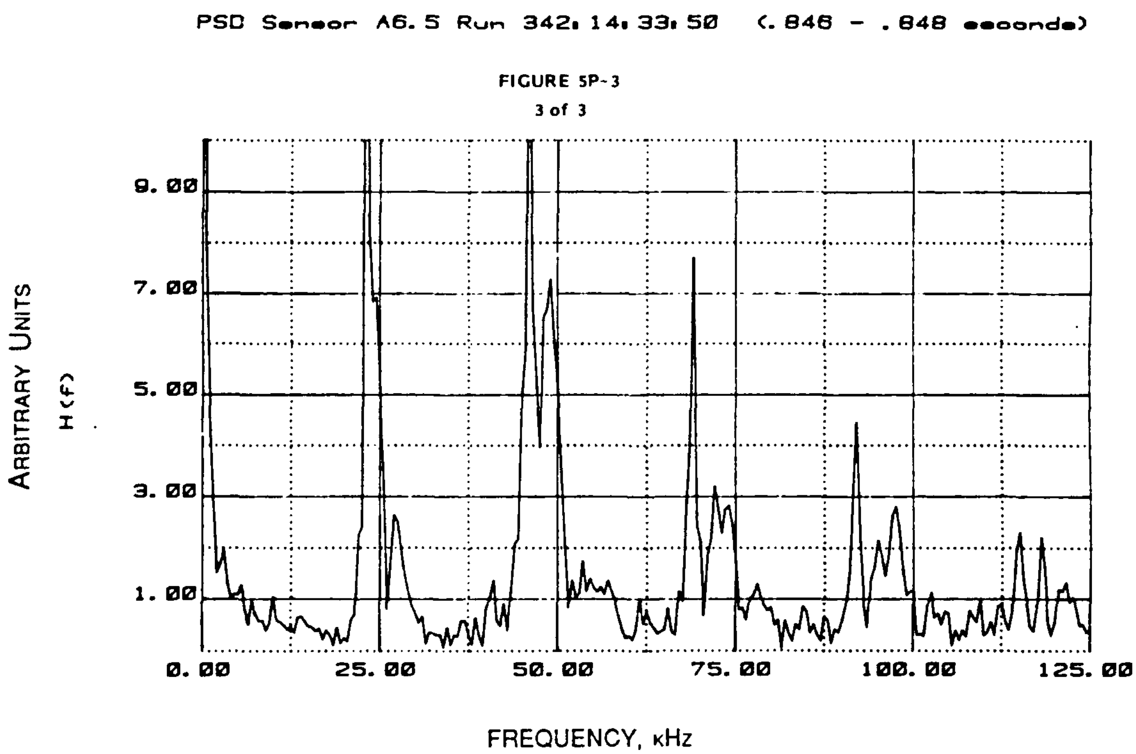

Figure 12. Frequency Analysis Plot, I.D. No. 342.14.33.50, From 846 to 848 ms.

2.2.3 Concept VI, 30 mm.

(1) Background. The 30-mm was tested at the General Electric test facility using Otto-II (Reeves 1985; Pate and Magoon 1985; Magoon et al. 1985) before shipment to the BRL. At BRL, tests were conducted using various HAN-based liquid propellants including NOS-365, LGP 1845, and LGP 1846 (Magoon et al. 1985; Watson et al. 1985, 1986; Watson, Knapton, and Klein 1987; Klingenberg et al. 1987). Instrumentation was similar to the tests performed with the 25-mm fixture. The tests reported here were all fired with charges of 80 or 160 cm^3 and an injection sheet thickness of 1.75 mm. The ballistic performance could possibly be improved using a thicker injection sheet, but this has not been tested. The nominal projectile mass was 287 g.

(2) Pressure Oscillations. Test firings performed both at the General Electric Ordnance Svstems Division and BRL produced pressure oscillations which have been interpreted in terms of acoustical oscillations. Some of the studies on the oscillations were summarized in Mandzy, Cushman, and Magoon (1984a); Magoon et al. (1985); and Watson et al. (1985).

A Fast Fourier Transform (FFT) plot of the data taken from Figure 2 is given in Figure 13. It was shown in Magoon et al. (1985) that the dominant frequency at 34.1 kHz could be matched with either one or two low-order modes (second radial or combined second radial-first tangential), assuming one could select a sound speed that was either 701 m/s or 914 m/s. Despite the relatively simple frequency content of the pressure record, an examination of the data did not identify a unique solution for the acoustical modes. The dominant frequency, as well as several of the other frequencies, could be identified with any one of several of the acoustical modes.

Interestingly, not all of the tests resulted in the simple frequency structure illustrated in Figures 2 and 13. In fact, most of the tests yielded rather complex frequency patterns. The results from one of the tests will be examined below in greater detail. The reason why a few of the tests resulted in a simple frequency pattern was not identified. One possible cause may have been related to the orientation of the crash ring in the combustion chamber.

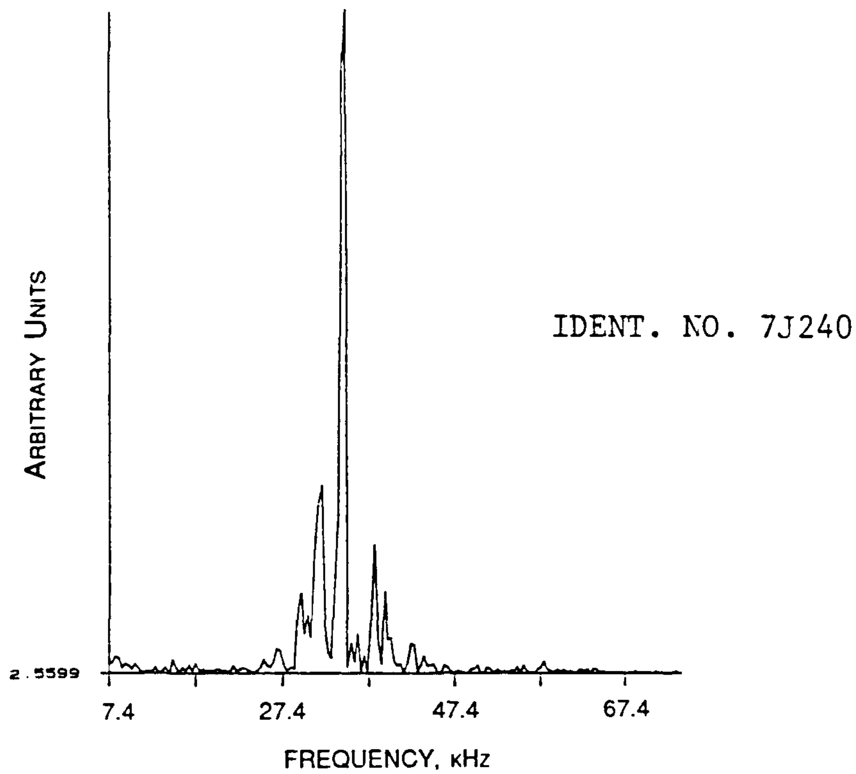

Figure 13. Fast Fourier Transform Plot of the Data Illustrated in Figure 2.

2.2.4 Concept VI, 105 mm.

(1) Test Conditions. The test conditions summarized here were fired with Otto-II. Instrumentation was similar to the tests performed with the 25-mm fixture. Two projectile masses were fired, 11.2 kg and 12.5 kg.

(2) Pressure Oscillations. A review of the pressure oscillations is given in Mandzy, Cushman, and Magoon (1984c); Mandzy et al. (1983); and Morrison and Knapton (1984). The data show very large-amplitude, high-frequency oscillations. The oscillations appear early in the test and continue well past completion of the injection. Typically, the frequencies of the oscillations in the 105-mm gun fixture are between 10–20 kHz, although the liquid-propellant gages also measured a 60-kHz oscillation of large amplitude. The frequencies are generally lower than in the 25-mm or 30-mm fixtures, as one would expect from the large chamber geometry in the 105-mm fixture. The amplitude of the pressure oscillations in the forward end of the chamber was about 50% of maximum pressure and was even higher towards the rear of the chamber. The oscillations started around 70 MPa. The frequencies of the oscillations

were characterized by a broad band of complex structures. Frequency analysis showed the existence of a band of frequencies between 13.8 and 15.3 kHz. Assuming a sound speed of 701 m/s (Grachis 1983; Cushman and Grachis 1983), the predicted acoustical frequencies are 13.9 kHz, 14.1 kHz, 14.5 kHz, and 15.2 kHz for the second radial, second radial-first tangential, second radial-second tangential, and second radial-third tangential modes, respectively. These frequencies were within ±200 Hz of the experimental frequencies identified from the frequency analysis study. Interestingly, there was no strong indication of the excitation of the first radial mode.

2.3 Sound Speed.

2.3.1 Thermodynamic Estimate. The estimates of the sound speed, including an arbitrary case where a 10% heat loss is assumed, are given in Table 2. The case for a 10% heat loss is based on assuming a 10% reduction in the gas-phase temperature. A lower gas-phase temperature seems reasonable based on closed-chamber temperatures measured by Klingenberg (1986).

2.3.2 Interior Ballistic Model. Coffee (1985) applied a lumped parameter interior ballistics model to the 30-mm Concept VI RLPG. Coffee's analyses were based on either an all-burnt condition immediately at injection or a jet break-up condition requiring a finite time for the combustion of the propellant. He computed a sound speed in the chamber using the two postulated combustion mechanisms. His results are summarized in Table 3 for the delayed burning-time case.

The results for the delayed-burning case are considered more reasonable (Coffee 1985) and result in a somewhat lower sound speed. The sound speed, c, for a two-phase flow, was calculated by Coffee (1987) using an equation derived by Wallis (1969):

$$c = \left(\frac{1}{\rho \left(\varepsilon / (\rho_g c_g^2) + (1 - \varepsilon) / (\rho_1 c_1^2) \right)} \right)^{1/2} ,$$

where

$$\varepsilon = \text{porosity} = \frac{V_g}{V_{ch}} ,$$

Table 2. Summary of Computed Gas-Phase Sound Speeds Obtained From a BLAKE Thermochemical Analysis (Freedman 1987)

Propellant	Case	Temperature, K	Gamma	Sound speed, m/s
Otto-II	No heat loss	1,986	1.272	1,311
1845	No heat loss	2,592	1.217	1,185
1846	No heat loss	2,469	1.218	1,183
Otto-II	Temp 10% less	1,787	1,261	1,226
1845	Temp 10% less	2,333	1.225	1,153
1846	Temp 10% less	2,222	1.232	1,134

Note: The estimated sound speeds for Otto-II and 1845 are also included for comparison purposes. The pressure for the no-heat-loss cases is 172 MPa.

Table 3. Predicted Sound Speeds for a 1/3 Charge Test With LGP 1846 for the Delayed-Burning Case (Coffee 1987)

Time, ms	Chamber pressure, MPa	Fraction burned	Sound speed, m/s
0.0	17	0.018	1,061
0.5	19	.020	1,050
1.0	22	.023	1,039
1.5	25	.026	1,032
2.0	29	.031	1,023
2.5	34	.036	1,010
3.0	40	.043	990
3.5	49	.053	960
4.0	60	.066	914
4.5	77	.087	859
5.0	90	.132	798
5.5	112	.260	835
6.0	149	.506	905
6.5	153	.780	972
7.0	121	.918	1,018
7.5	88	.968	999
8.0	65	.987	967

Note: Mean sound speed, 967 m/s; extremes, +94 m/s, -169 m/s.

$$c_1 = \left(\frac{K}{\rho_1}\right)^{1/2} ,$$

and

$$c_g = \left(\frac{\gamma p}{\rho_g(1 - b\rho_g)}\right)^{1/2} ,$$

where

ρ = mixture density
γ = specific heat ratio
V = volume
b = covolume
K = bulk modulus,

and the subscripts $_g$ and $_1$ refer to the gas and liquid phases, and $_{ch}$ refers to the chamber.

Figure 14, based on Coffee's model for the delayed-burning case, shows the computed sound speed and an estimate of the fraction burned. For comparison, a plot of the experimental data is shown in Figure 15 for both the pressure and piston displacement data as a function of time. A summary of the predicted sound speeds is given in Table 3.

3. EXPERIMENTAL

Two different crash rings, Figure 3, were used with the 30-mm tests performed at BRL. Only the results with the second or modified crash ring are reported here. The modified crash ring is a simpler design and may better satisfy the approximations used in the derivation of the eigenvalues summarized. The modified crash ring is attached to the front of the barrel face (Figure 1). The modified crash ring was designed with the baffle structure, which is illustrated for the normal crash ring in Figure 3.

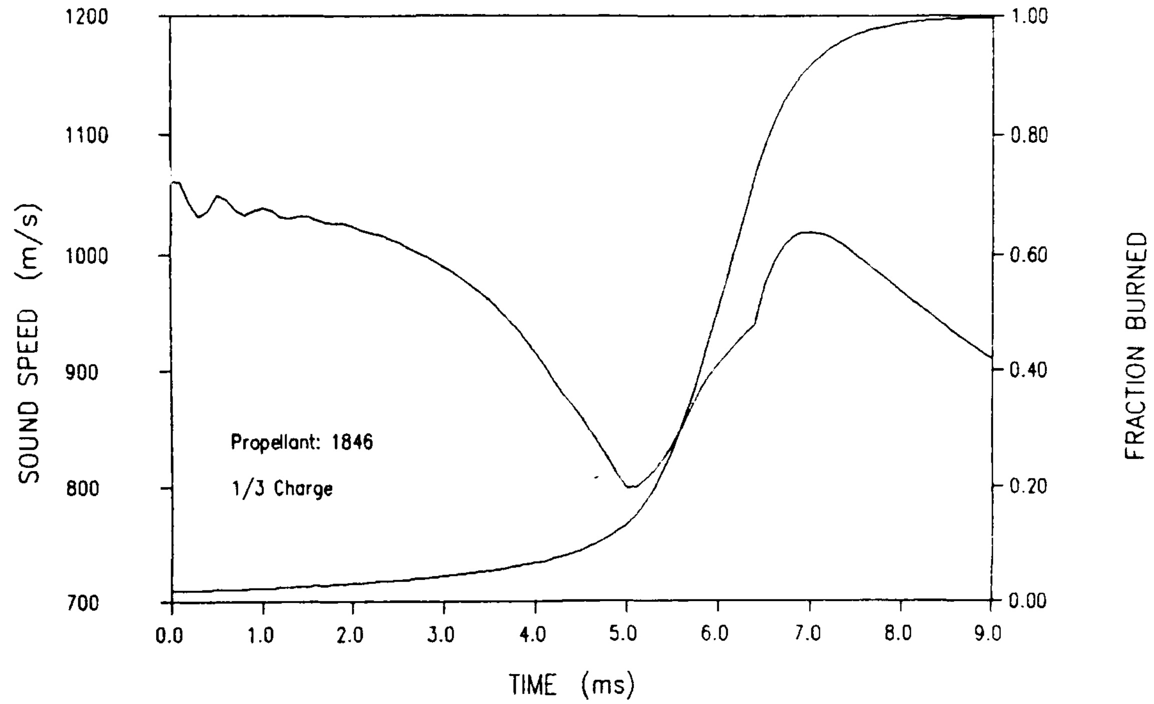

Figure 14. Estimated Sound Speed and the Fraction Burned for a Simulated 1/3 Charge With LGP 1846 (Based on the Coffee Model [Cushman and Grachis 1983; Klingenberg 1986]).

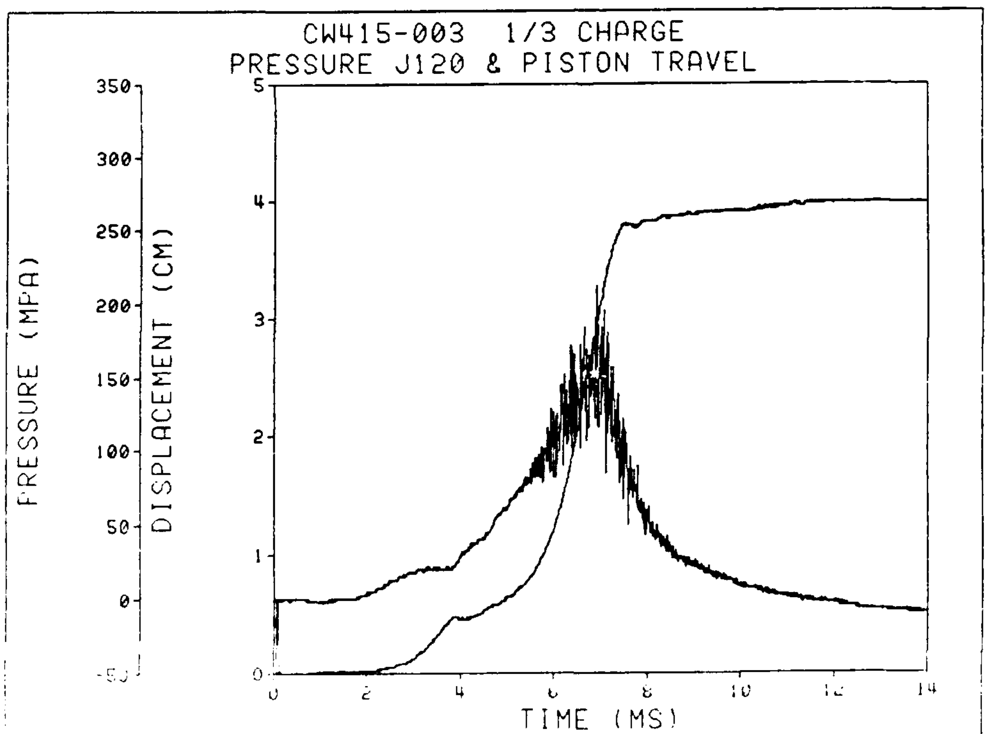

Figure 15. Pressure and Piston Displacement Data Based on a 1/3 Charge Test With LGP 1846 (I.D. No. 415-003).

Various propellant reservoir volumes are possible. This study reports only on the propellant volume at the 1/3 charge (80 cm^3). The initial volume in the combustion chamber with the modified crash ring was 145 cm^3. The liquid propellant used in the test was LGP 1846, and the nominal projectile mass was 287 g.

The pressure data are based on recordings at two locations in the combustion chamber, Figure 1. The forward gage in the J plane is 16 mm from the face of the barrel. The rear gage in the C plane is 54 mm from the face of the barrel. The initial position of the piston is 29 mm from the barrel face. The data were recorded using Kistler 607C4 pressure transducers.

Pressure data were recorded on an analog, magnetic tape recorder. The upper frequency cutoff of the recording system was about 80 kHz. However, frequencies above 50 to 60 kHz are questionable, since the limiting resonance frequency of the pressure gage cavity is approximately 62 kHz.

4. ANALYSIS

4.1 <u>Chamber Modes</u>. The analysis depends on taking FFTs of the pressure records to identify the frequency content of the data. Both the frequency and the relative magnitude of the FFT plots were determined.

The theoretical acoustical frequencies were determined using the eigenvalues computed by Cushman and Grachis (1983) for both a circular cavity and an annular cavity. The frequency of the modes was determined using the following:

$$f = \frac{ce}{2\pi r} ,$$

where c denotes the sound speed; e, the eigenvalue; and r, the inside radius of chamber, which equals 38.0 mm. The eigenvalues and the acoustical modes calculated by Grachis (1983) are given in Table 4.

Table 4. Eigenvalues and Acoustical Modes for a Circular Cavity and an Annular Cavity (Grachis 1983; Cushman and Grachis 1983)

Annular Chamber				Circular Chamber			
Eigenvalue[a]	Mode	Eigenvalue[a]	Mode	Eigenvalue	Mode	Eigenvalue	Mode
1.4332	1T	10.7000	9T	1.8412	1T	9.9695	2R2T
2.8034	2T	11.0126	2R	3.0542	2T	10.1735	3R
4.0773	3T	11.1248	2R1T	3.8317	1R	10.5199	1R5T
5.2642	4T	11.4579	2R2T	4.2012	3T	11.3459	2R3T
5.6098	1R	11.4816	1R6T	5.3176	4T	11.7060	3R1T
5.8486	1R1T	12.0028	2R3T	5.3314	1R1T	11.7349	1R6T
6.3945	5T	12.7477	2R4T	6.4156	5T	12.9324	1R7T
6.5290	1R2T	14.0385	1R8T	6.7061	1R2T	13.1704	3R2T
7.4933	6T	14.7789	2R6T	7.0156	2R	13.3237	4R
7.5550	1R3T	16.0126	2R7T	7.5013	6T	13.9872	2R5T
8.5749	7T	16.4552	3R	8.0152	1R3T	14.1155	1R8T
8.7985	1R4T	16.5284	3R1T	8.5363	2R1T	14.5858	3R3T
9.6464	8T	16.7468	3R2T	8.5778	7T	14.8636	4R1T
10.1370	1R5T	17.1073	3R3T	9.2824	1R7T	16.3475	4R2T
				9.6474	8T		

[a]The eigenvalues assume a value of 0.4254 for the ratio of the inner to outer radii of the chamber.

4.2 Comparison With Data. Whether the circular or the annular chamber is more appropriate for analyzing the pressure oscillations is subject to speculation. The circular chamber analysis might be more appropriate for the forward section of the chamber (J plane), and the annular chamber analysis (C plane) would be more appropriate for the rear of the chamber. In either case, it is conceivable that frequencies could be excited in both the rear and the forward section of the chamber. If so, the responses of the pressure gages could be influenced by frequencies excited in both sections of the chamber. The presence of the crash ring makes the analysis more difficult, especially in the forward section of the chamber. The crash ring used in the earlier tests introduced greater uncertainty in the results due to its more complex geometry. For this reason, the results summarized here are based only on the tests with the modified crash ring.

Some errors between the theoretical and the experimental acoustical modes are expected due to the complex flow processes. The theoretically predicted frequencies assume a continuous, homogeneous gas medium in a chamber with circular symmetry. The flow inside the combustion chamber may not be continuous or homogenous, but rather a turbulent, two-phase flow. Also, the actual configuration for the combustion chamber, which involves end effects, is different from the ideal case.

A value for the sound speed may be estimated by matching a particular acoustical mode with a frequency identified from an FFT plot. As will be shown, many sound speeds are indicated; whether they are of physical significance has to be examined in detail.

The example (I.D. 53) from a test with LGP 1846, given in Watson et al. (1985), is reexamined in this study. Pressure records, Figures 16 and 17, were given in Watson et al. (1985). The FFT data, Figures 18 and 19, are summarized in Tables 5 and 6, along with the assumed mode and the estimated sound speed. The forward portion of the combustion chamber with the modified crash ring more closely resembles a circular chamber than the rear section. Therefore, a better match between the observed frequencies and the theoretically predicted frequencies might be expected for the forward section of the chamber.

The superscript a in Tables 5 and 6 refers to a lack of a match between the experimental and predicted frequencies. Importantly, if a different sound speed had been selected, then a match would be possible. However, in most cases, a different experimental frequency would still be left without an assigned mode. Obviously, some judgment is required in the selection of the modes. Generally, the lower order modes were assigned to the frequencies with the larger relative magnitudes.

The 1/3 charge test with the modified crash ring yielded several frequencies with relatively large amplitudes. It was thought that the circular chamber analysis would be more appropriate for the response from the J gage. However, as shown in Table 5, the difference between the experimental and calculated frequencies, based on the circular chamber analysis, was rather large, especially for two of the low frequencies where it was not possible to obtain a good comparison. The fit of the data with the annular chamber analysis was somewhat better.

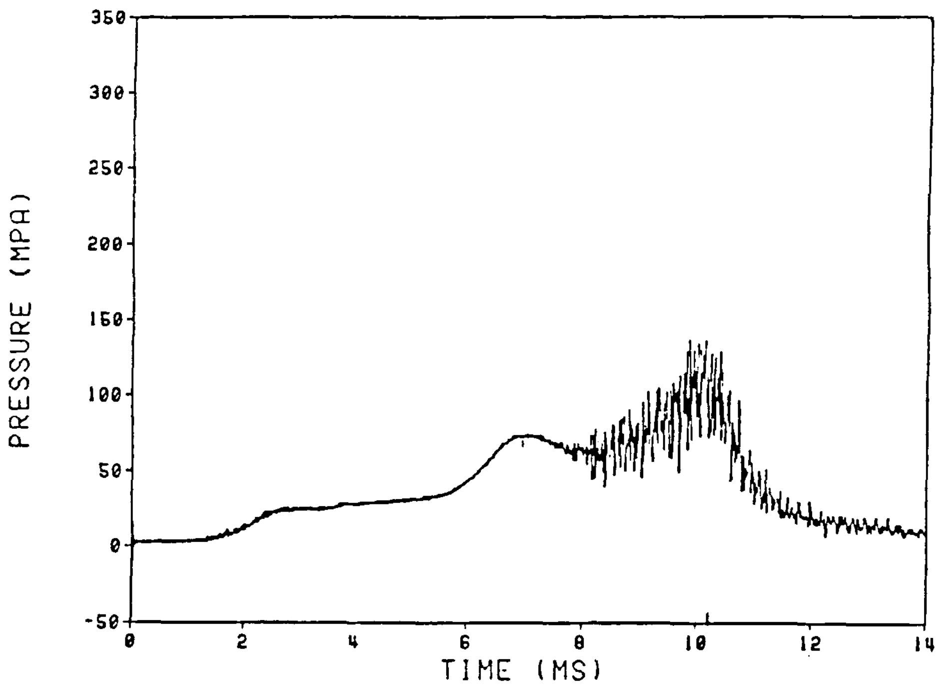

Figure 16. Pressure-Time Trace Recorded in Combustion Chamber, J Plane, for a 1/3 Charge Test With LGP 1846 (I.D. No. 53).

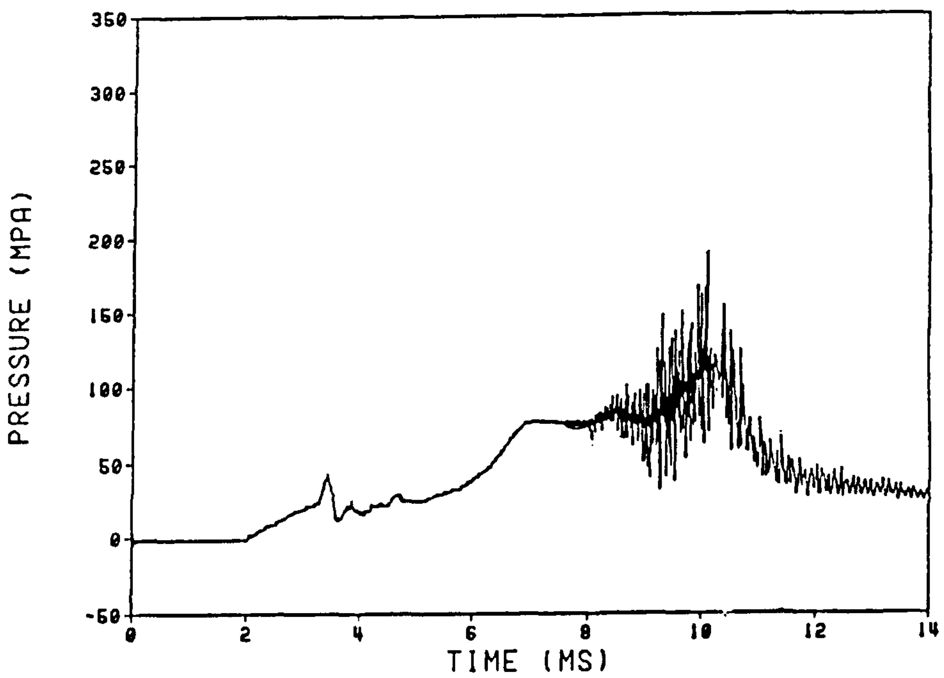

Figure 17. Pressure-Time Trace Recorded in Combustion Chamber, C Plane, for a 1/3 Charge Test With LGP 1846 (I.D. No. 53).

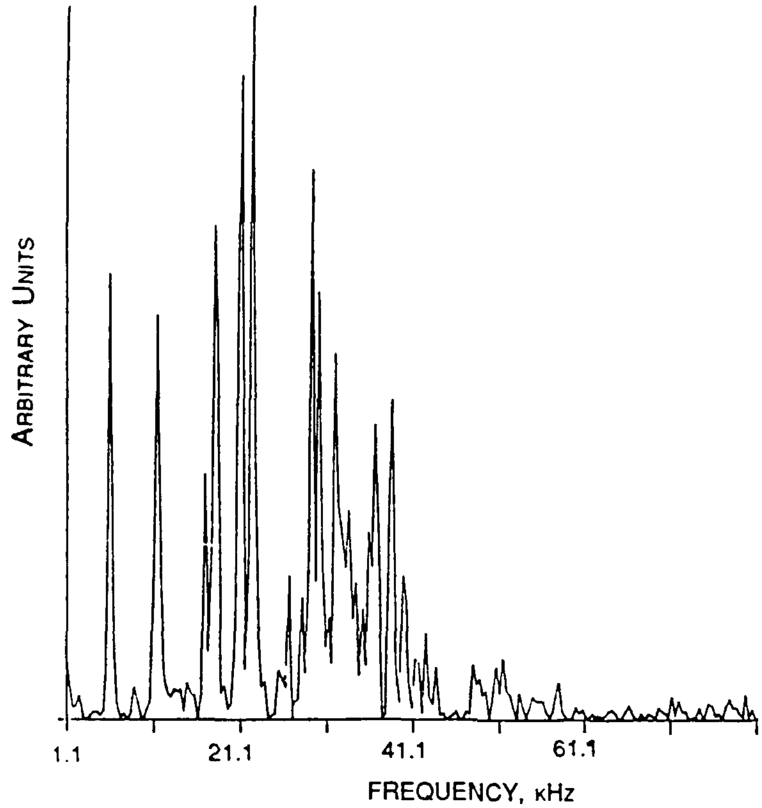

Figure 18. Fast Fourier Transform Plot of Test Illustrated in Figure 16, J Plane (I.D. No. 53).

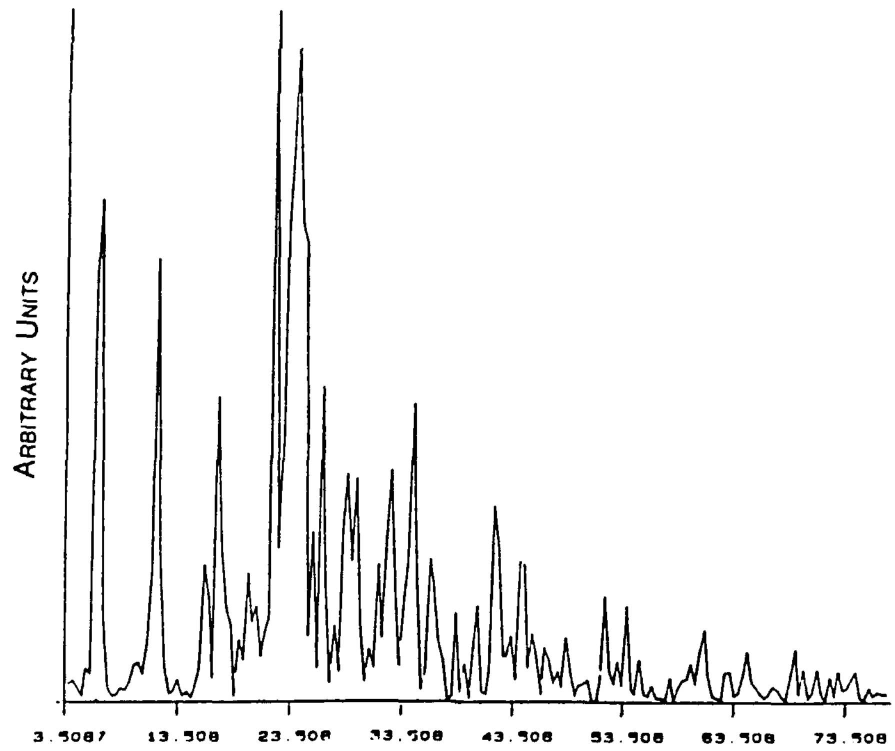

Figure 19. Fast Fourier Transform Plot of Test Illustrated in Figure 17, C Plane (I.D. No. 53).

Table 5. Summary of the FFT Frequencies and Estimate of Sound Speeds, Circular Chamber Analysis

Gage location	Fast Fourier Transform Plot: Relative amplitude	Frequency, kHz	Assumed mode	Sound speed, m/s
J	1.00	22.5	1R1T	1,010
J	0.90	21.1	—[a]	
J	0.77	29.4	1R2T	1,049
J	0.70	18.0	—[a]	
J	0.60	30.3	2R	1,034
J	0.57	11.7	2T	917
J	0.49	6.2	1T	806
J	0.45	38.8	1R4T	1,001
J	0.42	32.3	1R3T	965
J	0.41	36.8	2R1T	1,032
J	0.31	17.1	3T	974
C	1.00	22.2	1R1T	988
C	0.93	24.0	1R2T	857
C	0.72	6.4	1T	832
C	0.63	11.7	2T	917
C	0.45	26.3	2R	897
C	0.44	17.2	3T	980
C	0.42	34.5	2R1T	968

[a]No match between experimental frequency and an acoustical mode.

Note: The assumed modes are based on the circular chamber analysis. The test was I.D. No. 53 with a 1/3 charge of LGP 1846.

Table 6. Summary of the FFT Frequencies and Estimate of Sound Speeds, Annular Chamber Analysis

Gage location	Fast Fourier Transform Plot: Relative amplitude	Frequency, kHz	Assumed mode	Sound speed, m/s
J	1.00	22.5	1R	960
J	0.90	21.1	1R1T	864
J	0.77	29.4	1R2T	1,078
J	0.70	18.0	3T	1,057
J	0.60	30.3	—[a]	
J	0.57	11.7	2T	999
J	0.49	6.2	1T	1,036
J	0.45	38.8	1R4T	1,056
J	0.42	32.3	1R3T	1,023
J	0.41	36.8	—[a]	
J	0.31	17.1	4T	1,004
C	1.00	22.2	1R	947
C	0.93	24.0	1R1T	982
C	0.72	6.4	1T	1,069
C	0.63	11.7	2T	999
C	0.45	26.3	1R2T	964
C	0.44	17.2	3T	1,010
C	0.42	34.5	1R3T	1,093

[a]No match between experimental frequency and an acoustical mode.

Note: The assumed modes are based on the annular chamber analysis. The test was I.D. No. 53 with a 1/ charge of LGP 1846.

The sound speeds were calculated based on the assumption that the first low frequency matched the first tangential mode and that the dominant frequency with the largest relative amplitude could be matched with one of the low-order modes. Only the frequencies with the larger relative amplitudes are considered.

The mean sound speeds for the two groups of data summarized in Table 5 are 976 m/s and 920 m/s, with variations in the standard deviation of 7.8% and 6.7%, respectively.

The comparison of the FFT frequencies based on the annular chamber analysis is given in Table 6. The mean sound speeds for the two groups of data summarized in Table 6 are both 1,009 m/s, with variations in the standard deviation of 6.4% and 5.3%.

4.3 Waterfall Analysis. Waterfall plots were constructed for each record and are illustrated in Figures 20 and 21. The plots are produced b computing FFTs on short intervals of time and plotting the frequency spectrum along a baseline. The analysis is repeated over successive time intervals. The result is a plot of the frequency history of the record. One can distinguish between the longitudinal modes, if they exist, and the radial or tangential modes in the data by observing how the frequencies change with time. Longitudinal frequencies should decrease with time as the length of the chamber increases due to the piston and projectile motion. Radial and tangential modes remain more constant as the piston moves.

Results of the waterfall analysis show that the oscillations remain approximately constant during the main injection phase of the piston motion. There is no evidence of longitudinal modes in the chamber. The oscillations start, approximately, as the piston uncovers the minimum diameter portion of the center bolt and remain approximately constant until the piston stops. At that time, oscillations diminish or decrease rapidly with time.

5. CONCLUSIONS

For the two cases of interest, the calculated mean sound speeds for the annular chamber case and the circular chamber case are 1,009 m/s and 967 m/s, with standard deviations of 5.3% and 7.8%, respectively. These values compare with an averaged sound speed of 976 m/s, calculated from the Coffee model, assuming delayed burning. The differences in the

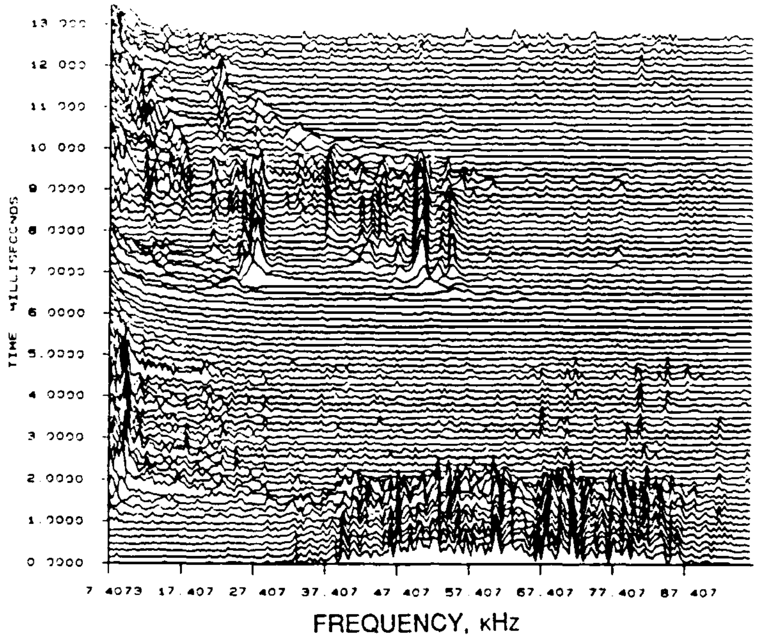

Figure 20. <u>Waterfall Plot for J Plane (I.D. No. 53)</u>.

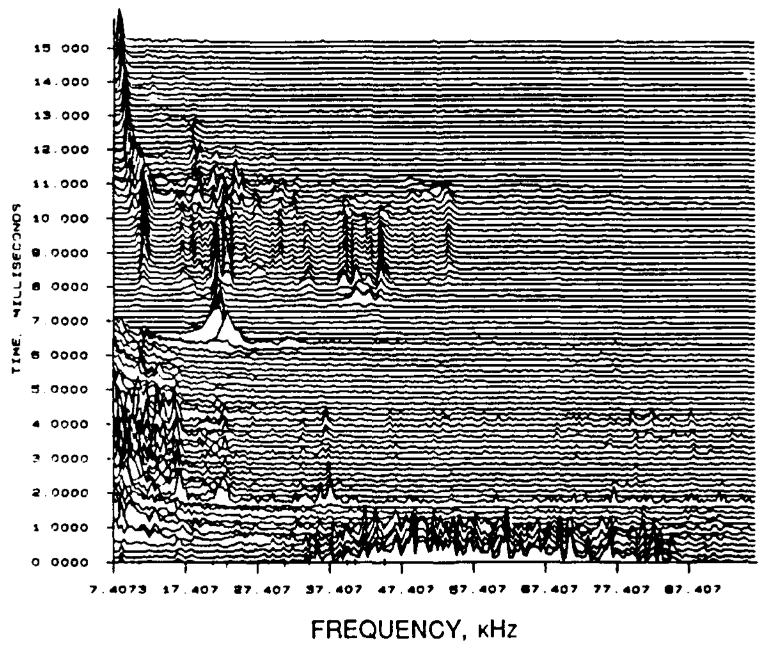

Figure 21. <u>Waterfall Plot for C Plane (I.D. No. 53)</u>.

sound speed determined by the two methods are 4.3% and 1.0%, respectively. The agreement is reasonably good when considering the assumptions used in the analysis and gives additional support to the postulate that at least some of the observed experimental frequencies may be attributed to the excitation of the acoustical modes.

Importantly, the FFTs of the data identified some frequencies that were difficult to assign to a particular acoustical mode. This suggests that there may be some frequencies that cannot be attributed to an acoustical chamber frequency. Two examples are given in Table 5 for the data recorded at the J plane, indicating frequencies at 18.0 kHz and 21.1 kHz that were not assigned to one of the acoustical modes.

Results of the waterfall analysis show that the oscillations remain approximately constant during the combustion. We conclude, therefore, that the pressure oscillations are tangential and/or radial modes. Also, there is no strong evidence of longitudinal modes in the chamber indicated in the analysis.

Although not a subject of this paper, the experimental approaches for reducing or eliminating the oscillations fall into two categories. The first category consists of approaches to remove the driving force from the system. This may be difficult if the source is an integral part of the process. Interestingly, in one concept, similar to the concept studied in this paper and referred to as Concept VIA, there was a significant reduction in the amplitude of the oscillations. In Concept VIA, the injection orifice contours were varied, and, in one configuration, the amplitude of the oscillations was reduced.

The second category consists of approaches to make the system unfavorable to sustain the oscillations. Rocket engineers use baffles and acoustical liners in the engines to control instabilities. Baffles and acoustic liners might be installed in a gun, although the conditions in a gun, due to the high pressures, may limit the practicality of such an approach (Hasenbein 1981).

6. REFERENCES

Coffee, T. "A Lumped Parameter Code for Regenerative Liquid Propellant Guns." BRL-TR-2703, U.S. Army Ballistic Research Laboratory, Aberdeen Proving Ground, MD, December 1985.

Coffee, T. "The Analysis of Experimental Measurements on Liquid Propellant Guns." BRL-TR-2731, U.S. Army Ballistic Research Laboratory, Aberdeen Proving Ground, MD, May 1986.

Coffee, T. Private communication to J. D. Knapton. U.S. Army Ballistic Research Laboratory, Aberdeen Proving Ground, MD, June 1987.

Cushman, P. G., and G. Grachis. "Linear Wave Motion in the Concept VI Liquid Propellant Test Fixture." General Electric Ordnance Systems Division, unpublished report, November 1983.

Freedman, E. Private communication to J. D. Knapton. U.S. Army Ballistic Research Laboratory, Aberdeen Proving Ground, MD, January 1987.

Grachis, G. "Estimate of the Speed of Sound in the 105-mm Concept VI Test Fixture." General Electric Ordnance Systems Division, unpublished report, February 14, 1983.

Graham, A. R. "The Regenerative Liquid Propellant Gun." <u>Chemical Propulsion Information Agency Publication No. 366</u>, vol. 2, pp. 261–303, October 1982.

Graham, A. R. "Design Study for a 40-mm Regenerative Combustion Liquid Propellant Test Fixture." Mechanical Technology, Inc., MTI G7-580, December 16, 1987.

Graham, A. R., and M. J. Bulman. "General Electric 25-mm Regenerative Liquid Propellant Gun Program." <u>Chemical Propulsion Information Agency Publication No. 273</u>, vol. 1, pp. 391–404, August 1975.

Hasenbein, R. G. "Regenerative Liquid Propellant Gun Technology." ARLCB-TR-81026, Benet Weapons Laboratory, Watervliet, NY, June 1981.

Juhasz, A. Private communication to J. D. Knapton. U.S. Army Ballistic Research Laboratory, Aberdeen Proving Ground, MD, 1987.

Kent, R. H. "Report on Determination of Interior Ballistic Data by Closed Chamber Experiments in Connection with Project RB 158." BRL-R-32, U.S. Army Ballistic Research Laboratory, Aberdeen Proving Ground, MD, January 1936.

Klingenberg, G. "Closed Bomb Studies of the Liquid Gun Propellant 1845." Fraunhofer-Institute für Kurzzeitdynamik, Ernst-Mach-Institut, Report 1/86, April 1986.

Klingenberg, G., J. D. Knapton, W. F. Morrison, and C. A. Watson. "Liquid Gun Propellant Studies: Closed Bomb and Gun Studies." Proceedings of the 10th International Symposium on Ballistics, vol. 1, American Defense Preparedness Association, San Diego, CA, October 1987.

Magoon, I., J. Mandzy, C. A. Watson, J. DeSpirito, and J. D. Knapton. "Test Data from a Regenerative Sheet Type of Liquid Propellant Gun." Chemical Propulsion Information Agency Publication 432, vol. 2, pp. 225–238, October 1985.

Mandzy, J., P. G. Cushman, and I. Magoon. "Liquid Propellant Final Report." General Electric Ordnance Systems Division, Pittsfield, MA, August 1984a (Contract No. DAAK11-78-C-0054, also published as BRL-CR-546, October 1985).

Mandzy, J., P. G. Cushman, and I. Magoon. Technical Notes on Concept V Evaluation. General Electric Ordnance Systems Division, Pittsfield, MA, August 1984b (Contract No. DAAK11-78-C-0054, also published as BRL-CR-560 September 1986).

Mandzy, J., P. G. Cushman, and I. Magoon. "Technical Notes on Concept VI 105-mm Evaluation." General Electric Ordnance Systems Division, August 1984c (Contract No. DAAK11-78-C-0054, also published as BRL-CR-579, August 1987).

Mandzy, J., P. G. Cushman, and I. Magoon. "Technical Notes on Scaling Investigation of Concept VI." General Electric Ordnance Systems Division, Pittsfield, MA, August 1984d (Contract No. DAAK11-78-C-0054, also published as a BRL-CR-580, August 1987).

Mandzy, J., I. Magoon, W. F. Morrison, and J. D. Knapton. "Preliminary Report on Test Firings of a 105-mm Regenerative Fixture." Chemical Propulsion Information Agency Publication 383, vol. 2, pp. 161–172, October 1983.

Morrison, W. F., and J. D. Knapton. "Firing Results from a 105-mm Regenerative Liquid Propellant Gun." Third International Gun Propulsion Symposium, Edited by J. P. Picard and S. Nicolaides, American Defense Preparedness Association, vol. 2, pp. 123–141, November 1984.

Pate, R., and I. Magoon. "Preliminary Results from Ballistic Investigations in 30-mm Regenerative Liquid Propellant Gun Firings." Chemical Propulsion Information Agency Publication 432, vol. 2, pp. 213–224, October 1985.

Reeves, K. P. "Operating Manual and Final Test Report for the 30-mm BRL Regenerative Liquid Propellant Test Fixture." General Electric Ordnance Systems Division, October 1985 (Contract No. DAAK 11-83-C-0007).

Wallis, G. B. One-Dimensional Two-Phase Flow. New York: McGraw-Hill, Inc., pp. 139–144, 1969.

Watson, C. A., J. D. Knapton, N. Boyer, I. C. Stobie, and M. M. Decker. "The Ballistic Characteristics of Contaminated Liquid Propellants in a 30-mm Regenerative Liquid Propellant Gun." Chemical Propulsion Information Agency Publication 457, vol. 2, pp. 539–549, October 1986.

Watson, C. A., J. D. Knapton, J. DeSpirito, and N. Boyer. "A Study on High Frequency Oscillations Observed in a 30-mm Regenerative Liquid Propellant Gun." Chemical Propulsion Information Agency Publication 432, vol. 2, pp. 239–254, October 1985.

Watson, C. A., J. D. Knapton, and N. Klein. "Sensitivity of Regenerative Liquid Propellant Gun Interior Ballistics on Variations in the Propellant Oxidizer to Fuel Ratio." Chemical Propulsion Information Agency Publication 476, vol. 3, pp. 391–394, October 1987.

INTENTIONALLY LEFT BLANK.

No. of Copies	Organization
2	Administrator Defense Technical Info Center ATTN: DTIC-DDA Cameron Station Alexandria, VA 22304-6145
1	Commander U.S. Army Materiel Command ATTN: AMCAM 5001 Eisenhower Avenue Alexandria, VA 22333-0001
1	Commander U.S. Army Laboratory Command ATTN: AMSLC-DL 2800 Powder Mill Road Adelphi, MD 20783-1145
2	Commander U.S. Army Armament Research, Development, and Engineering Center ATTN: SMCAR-IMI-I Picatinny Arsenal, NJ 07806-5000
2	Commander U.S. Army Armament Research, Development, and Engineering Center ATTN: SMCAR-TDC Picatinny Arsenal, NJ 07806-5000
1	Director Benet Weapons Laboratory U.S. Army Armament Research, Development, and Engineering Center ATTN: SMCAR-CCB-TL Watervliet, NY 12189-4050
(Unclass. only)1	Commander U.S. Army Armament, Munitions and Chemical Command ATTN: AMSMC-IMF-L Rock Island, IL 61299-5000
1	Director U.S. Army Aviation Research and Technology Activity ATTN: SAVRT-R (Library) M/S 219-3 Ames Research Center Moffett Field, CA 94035-1000

No. of Copies	Organization
1	Commander U.S. Army Missile Command ATTN: AMSMI-RD-CS-R (DOC) Redstone Arsenal, AL 35898-5010
1	Commander U.S. Army Tank-Automotive Command ATTN: ASQNC-TAC-DIT (Technical Information Center) Warren, MI 48397-5000
1	Director U.S. Army TRADOC Analysis Command ATTN: ATRC-WSR White Sands Missile Range, NM 88002-5502
1	Commandant U.S. Army Field Artillery School ATTN: ATSF-CSI Ft. Sill, OK 73503-5000
(Class. only)1	Commandant U.S. Army Infantry School ATTN: ATSH-CD (Security Mgr.) Fort Benning, GA 31905-5660
(Unclass. only)1	Commandant U.S. Army Infantry School ATTN: ATSH-CD-CSO-OR Fort Benning, GA 31905-5660
1	Air Force Armament Laboratory ATTN: WL/MNOI Eglin AFB, FL 32542-5000
	<u>Aberdeen Proving Ground</u>
2	Dir, USAMSAA ATTN: AMXSY-D AMXSY-MP, H. Cohen
1	Cdr, USATECOM ATTN: AMSTE-TC
3	Cdr, CRDEC, AMCCOM ATTN: SMCCR-RSP-A SMCCR-MU SMCCR-MSI
1	Dir, VLAMO ATTN: AMSLC-VL-D
10	Dir, BRL ATTN: SLCBR-DD-T

No. of Copies	Organization
2	Director Defense Advanced Research Projects Agency ATTN: J. Lupo J. Richardson 1400 Wilson Boulevard Arlington, VA 22209
1	HQ, U.S. Army Materiel Command ATTN: AMCICP-AD, B. Dunetz 5001 Eisenhower Avenue Alexandria, VA 22333-0001
7	Commander U.S. Army Armament Research, Development, and Engineering Center ATTN: SMCAR-AEE-BR, B. Brodman W. Seals A. Beardell SMCAR-AEE-B, D. Downs SMCAR-AEE-W, N. Slagg SMCAR-AEE, A. Bracuti J. Lannon Picatinny Arsenal, NJ 07806-5000
2	Commander U.S. Army Armament Research, Development, and Engineering Center ATTN: SMCAR-FSS-D, L. Frauen SMCAR-FSA-S, H. Liberman Picatinny Arsenal, NJ 07806-5000
4	Commander U.S. Army Armament Research, Development, and Engineering Center ATTN: SMCAR-FSS-DA, Bldg 94 J. Feneck R. Kopmann J. Irizarry M. Oetken Picatinny Arsenal, NJ 07806-5000
2	Commandant U.S. Army Field Artillery School ATTN: ATSF-CMW ATSF-TSM-CN, J. Spicer Fort Sill, OK 73503

No. of Copies	Organization
4	Director Benet Weapons Laboratory U.S. Army Armament Research, Development, and Engineering Center ATTN: SMCAR-CCB-DS, E. Conroy A. Graham SMCAR-CCB, L. Johnson SMCAR-CCB-S F. Heiser Watervliet, NY 12189-4050
1	Commander Materials Technology Laboratory U.S. Army Laboratory Command ATTN: SLCMT-MCM-SB, M. Levy Watertown, MA 02172-0001
1	Commander, USACECOM R&D Technical Library ATTN: ASQNC-ELC-IS-L-R, Myer Center Ft. Monmouth, NJ 07703-5000
1	Commander U.S. Army Laboratory Command ATTN: SLCHD-TA-L 2800 Powder Mill Rd Adelphi, MD 20783-1145
1	Commander U.S. Army Belvoir RD&E Center ATTN: STRBE-WC, Tech Library (Vault) B-315 Fort Belvoir, VA 22060-5606
1	Commander U.S. Army Research Office ATTN: Technical Library P.O. Box 12211 Research Triangle Park, NC 27709-2211
1	Commander U.S. Army Armament Research, Development, and Engineering Center ATTN: SMCAR-CCS-C, T. Hung Picatinny Arsenal, NJ 07806-5000
1	Commandant U.S. Army Armor Center ATTN: ATSB-CD-MLD Fort Knox, KY 40121

No. of Copies	Organization
1	Commander Naval Surface Warfare Center ATTN: D. A. Wilson, Code G31 Dahlgren, VA 22448-5000
1	Commander Naval Surface Warfare Center ATTN: J. East, Code G33 Dahlgren, VA 22448-5000
2	Commander Naval Surface Warfare Center ATTN: O. Dengel K. Thorsted Silver Spring, MD 20902-5000
1	Commander (Code 3247) Naval Weapons Center Guns Systems Branch China Lake, CA 93555-6001
1	OSD/SDIO/IST ATTN: Dr. Len Caveny Pentagon Washington, DC 20301-7100
1	Commandant USAFAS ATTN: ATSF-TSM-CN Fort Sill, OK 73503-5600
1	Director Jet Propulsion Laboratory ATTN: Technical Library 4800 Oak Grove Drive Pasadena, CA 91109
1	IITRI ATTN: Library 10 W. 35th St Chicago, IL 60616
1	Olin Chemicals Research ATTN: David Gavin PO Box 586 Chesire, CT 06410-0586
2	Olin Corporation ATTN: Victor A. Corso Dr. Ronald L. Dotson 24 Science Park New Haven, CT 06511
2	National Aeronautics and Space Administration ATTN: MS-603, Technical Library MS-86, Dr. Povinelli 21000 Brookpark Road Lewis Research Center Cleveland, OH 44135
1	Director National Aeronautics and Space Administration Manned Spacecraft Center Houston, TX 77058
10	Central Intelligence Agency Office of Central Reference Dissemination Branch Room GE-47 HQS Washington, DC 20502
1	Central Intelligence Agency ATTN: Joseph E. Backofen HQ Room 5F22 Washington, DC 20505
1	Calspan Corporation ATTN: Technical Library PO Box 400 Buffalo, NY 14225
6	General Electric Ord Sys Div ATTN: J. Mandzy, OP43-220 R. E. Mayer H. West W. Pasko R. Pate I. Magoon 100 Plastics Avenue Pittsfield, MA 01201-3698
1	General Electric Company Armament Systems Department ATTN: D. Maher Burlington, VT 05401

No. of Copies	Organization
1	Alliant Techsystems, Inc. ATTN: R. E. Tompkins MN38-3300 10400 Yellow Circle Drive Minnetonka, MN 55343
1	Paul Gough Associates, Inc. ATTN: Dr. Paul S. Gough 1048 South Street Portsmouth, NH 03801-5423
1	Safety Consulting Engineering ATTN: Mr. C. James Dahn 5240 Pearl St. Rosemont, IL 60018
1	Science Applications, Inc. ATTN: R. Edelman 23146 Cumorah Crest Woodland Hills, CA 91364
2	Science Applications International Corporation ATTN: Dr. F. T. Phillips Dr. Fred Su 10210 Campus Point Drive San Diego, CA 92121
1	Science Applications International Corporation ATTN: Norman Banks 4900 Waters Edge Drive Suite 255 Raleigh, NC 27606
1	Sundstrand Aviation Operations ATTN: Mr. Owen Briles PO Box 7202 Rockford, IL 61125
1	Veritay Technology, Inc. ATTN: E. B. Fisher 4845 Millersport Highway PO Box 305 East Amherst, NY 14051-0305

No. of Copies	Organization
1	Director Applied Physics Laboratory The Johns Hopkins University Johns Hopkins Road Laurel, MD 20707
2	Director CPIA The Johns Hopkins University ATTN: T. Christian Technical Library Johns Hopkins Road Laurel, MD 20707
1	University of Illinois at Chicago ATTN: Professor Sohail Murad Department of Chemical Engineering Box 4348 Chicago, IL 60680
1	University of Maryland at College Park ATTN: Professor Franz Kasler Department of Chemistry College Park, MD 20742
1	University of Missouri at Columbia ATTN: Professor R. Thompson Department of Chemistry Columbia, MO 65211
1	University of Michigan ATTN: Professor Gerard M. Faeth Department of Aerospace Engineering Ann Arbor, MI 48109-3796
1	University of Missouri at Columbia ATTN: Professor F. K. Ross Research Reactor Columbia, MO 65211
1	University of Missouri at Kansas City Department of Physics ATTN: Professor R. D. Murphy 1110 East 48th Street Kansas City, MO 64110-2499

No. of Copies	Organization
1	Pennsylvania State University Department of Mechanical Engineering ATTN: Professor K. Kuo University Park, PA 16802
2	Princeton Combustion Research Laboratories, Inc. ATTN: N. A. Messina M. Summerfield 4275 U.S. Highway One North Monmouth Junction, NJ 08852
1	University of Arkansas Department of Chemical Engineering ATTN: J. Havens 227 Engineering Building Fayetteville, AR 72701
3	University of Delaware Department of Chemistry ATTN: Mr. James Cronin Professor Thomas Brill Mr. Peter Spohn Newark, DE 19711
1	University of Texas at Austin Bureau of Engineering Research ATTN: BRC EME133, Room 1.100 H. Fair 10100 Burnet Road Austin, TX 78758

INTENTIONALLY LEFT BLANK.

USER EVALUATION SHEET/CHANGE OF ADDRESS

This laboratory undertakes a continuing effort to improve the quality of the reports it publishes. Your comments/answers below will aid us in our efforts.

1. Does this report satisfy a need? (Comment on purpose, related project, or other area of interest for which the report will be used.) ______________________

2. How, specifically, is the report being used? (Information source, design data, procedure, source of ideas, etc.) ______________________

3. Has the information in this report led to any quantitative savings as far as man-hours or dollars saved, operating costs avoided, or efficiencies achieved, etc? If so, please elaborate. ______________________

4. General Comments. What do you think should be changed to improve future reports? (Indicate changes to organization, technical content, format, etc.) ______________________

BRL Report Number BRL-TR-3322 Division Symbol ______________

Check here if desire to be removed from distribution list. ____

Check here for address change. ____

Current address: Organization ______________
Address ______________

DEPARTMENT OF THE ARMY
Director
U.S. Army Ballistic Research Laboratory
ATTN: SLCBR-DD-T
Aberdeen Proving Ground, MD 21005-5066

OFFICIAL BUSINESS

BUSINESS REPLY MAIL
FIRST CLASS PERMIT No 0001, APG, MD

Postage will be paid by addressee.

NO POSTAGE NECESSARY IF MAILED IN THE UNITED STATES

Director
U.S. Army Ballistic Research Laboratory
ATTN: SLCBR-DD-T
Aberdeen Proving Ground, MD 21005-5066